Supporting Information

Title Employing a Similar Acceptor Material as Third Component to Enhance the Performance of Organic Solar Cells

Kun Wang, Haolei Bai, Cheng Zhang, Chunxiao Sun, Shuyang Sang, Yuechen Li, Zekun Chen, Jia'nan Hu, Xiaojun Li, Lei Meng*, Yongfang Li*

Dr. Kun Wang, Haolei Bai, Cheng Zhang, Chunxiao Sun, Jia'nan Hu
School of Materials and Chemical Engineering, Zhongyuan University of Technology, Zhengzhou, 451191, China
E-mail: (kwang@zut.edu.cn)

Cheng Zhang, Shuyang Sang, Yuechen Li, Zekun Chen, Prof. Xiaojun Li, Prof. Lei Meng, Prof. Yongfang Li
Beijing National Laboratory for Molecular Sciences, CAS Key Laboratory of Organic Solids, Institute of Chemistry, Chinese Academy of Sciences, Beijing, 100190, China
E-mail: (menglei@iccas.ac.cn)

Experimental section

1. Materials.

All chemicals and solvents were of reagent grade and were purchased from Alfa Aesar, J&K and Aldrich, respectively. The molecular structures and synthetic routes of **Y-TNF** and **Y-TN** are shown in **Scheme S1** and **Scheme S2**, as follows:

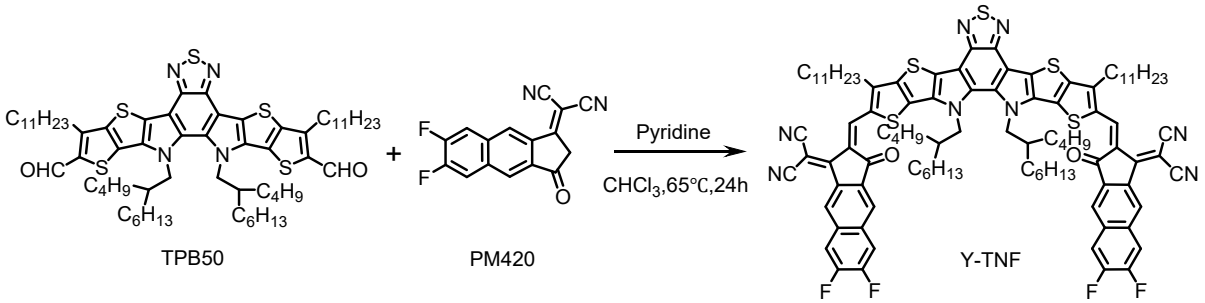

Scheme S1. The synthetic route and molecular structure of **Y-TNF**.

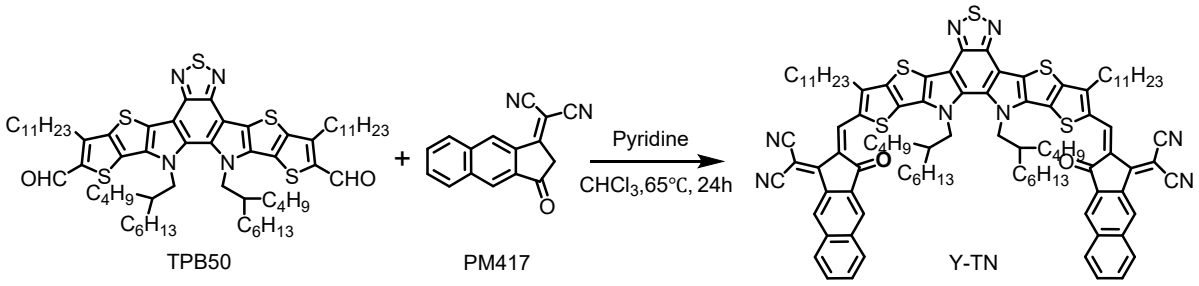

Scheme S2. The synthetic route and molecular structure of **Y-TN**.

2. Instruments and measurements

^{1}H NMR and ^{13}C NMR were measured in $CDCl_3$ on Bruker AV 400 MHz FT-NMR spectrometer. MALDI-TOF was measured on ultrafleXtreme™ Mass spectrometer from Bruker Daltonics. UV-Vis absorption spectra were measured by an Agilent Carry-5000 UV-Vis spectrophotometer. Electrochemical cyclic voltammetry (CV) was performed on a Zahner Zennium IM6 electrochemical workstation with a three-electrode system in 0.1 mol L^{-1} Bu_4NPF_6 acetonitrile solutions at a scan rate of 50 mV s^{-1}. The atomic force microscopy (AFM) measurement was carried out on a Dimension 3100 (Veeco) Atomic Force Microscope in the tapping mode. Transmission electron microscopy (TEM) was performed on a Japanese JEOL JEM-F200 instrument at 200 kV accelerating voltage. The GWAXS measurements were performed at beamline 7.3.3 at the Advanced Light Source (ALS). The current-voltage (*J-V*) characteristics of the devices were measured on a Keithley 2450 Source Measure Unit. The power conversion efficiency of the OSCs was measured under an illumination of AM 1.5 G (100 mW cm^{-2}) using a SS-F5-3A (Enli Technology Co. Ltd.) solar simulator (AAA grade, 50 mm x 50 mm photobeam size). The EQE was measured by Solar Cell Spectral Response Measurement System QE-R3011 (Enli Technololy Co. Ltd.). The light intensity at each wavelength was calibrated with a standard single-crystal Si photovoltaic cell. The data of transient photocurrent (TPC), transient photovoltage (TPV), and photoinduced chargecarrier extraction by linearly increasing voltage (Photo-CELIV) were obtained by the all-in-one characterization platform, Paios (Fluxim AG, Switzerland). In TPC testing, the light intensities

were10%, 17.8%, 31.6%, 56.2%, and 100% sunlight, respectively. The settling time was 100 μs, pulse length was 100 μs and the follow-up time was 200 μs. In the TPV testing, the light intensities were 0.10%, 0.23%, 0.53%, 1.23%, 2.83%, 6.52%, 15.0%, 34.6%, and 80.0% sunlight, respectively. The settling time was 30 ms, pulse length was 5 ms and the follow-up time was 30 μs. In the Photo-CLIVE testing, the delay time was set to 0 s, the light intensity was 100% sunlight, the light-pulse length was 100 μs, and the sweep ramp rate increased from 20 V ms^{-1} to 100 V ms^{-1}.

3. Device fabrication method

The OSC devices were fabricated with the ITO/PEDOT:PSS/PM6:Y-TN or PM6:Y-TNF:Y-TN/PDINN/Ag (100 nm) structure. Prior to fabrication, the ITO-coated glass substrate was cleaned with deionized water, acetone, and isopropanol. Afterwards, the substrate was treated with UV-ozone for 30 minutes. The PEDOT:PSS was spin-coated onto the ITO-coated glass surface at a spinning rate of 7000 rpm for 30 seconds. It was then dried at 150°C for 30 minutes and transferred into a nitrogen glove box with less than 5 ppm oxygen and moisture. The active layer was deposited onto the PEDOT:PSS layer by spin-coating a trichloromethane solution of PM6:Y-TNF/PM6:Y-TNF:Y-TN with a blend concentration of 18.4 mg mL^{-1}. The PDINN solution, with a concentration of 1 mg mL^{-1} in methanol, was spin-coated onto the surface of the ITO-coated active layer at 3000 rpm for 30 seconds. Subsequently, 100 nm of Ag was evaporated onto the active layer in a vacuum chamber under a pressure of approximately 4×10^{-4} Pa.

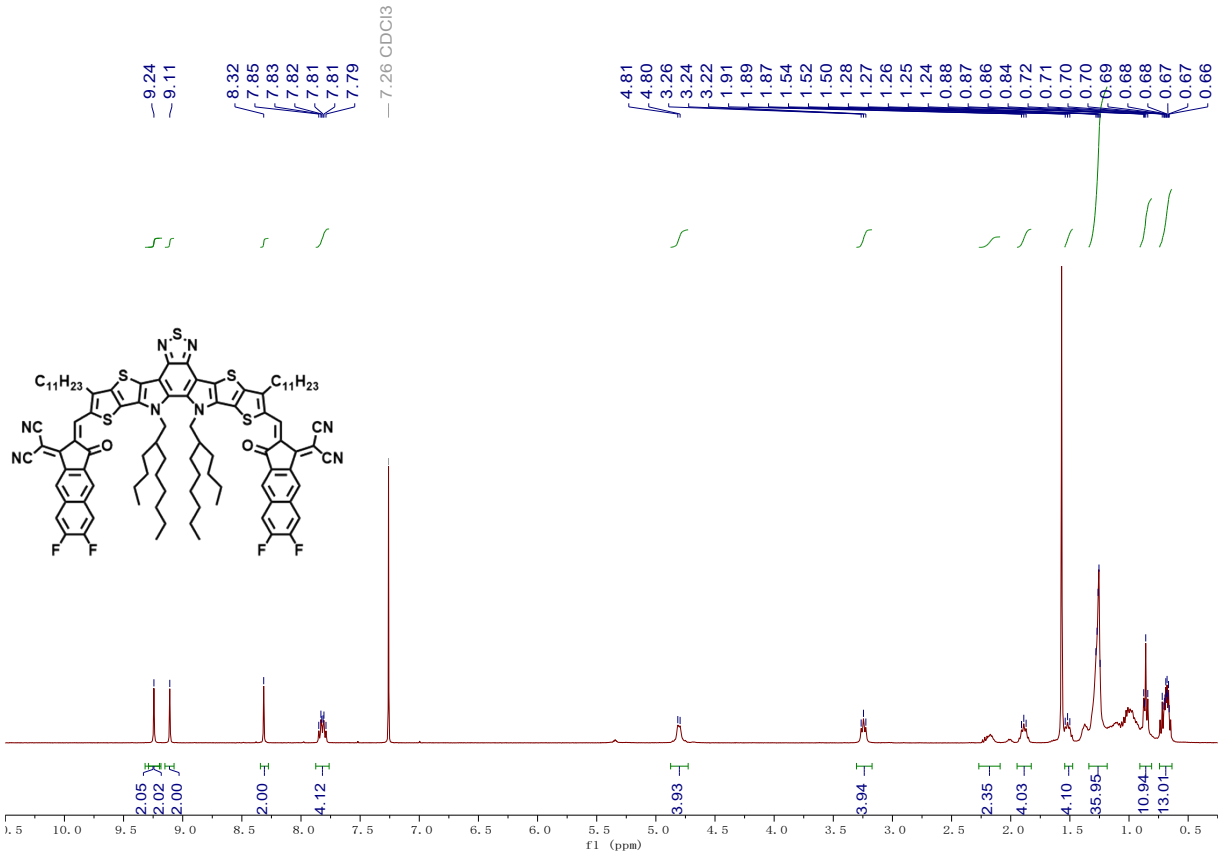

Figure S1. ^{1}H NMR of Y-TNF in $CDCl_3$.

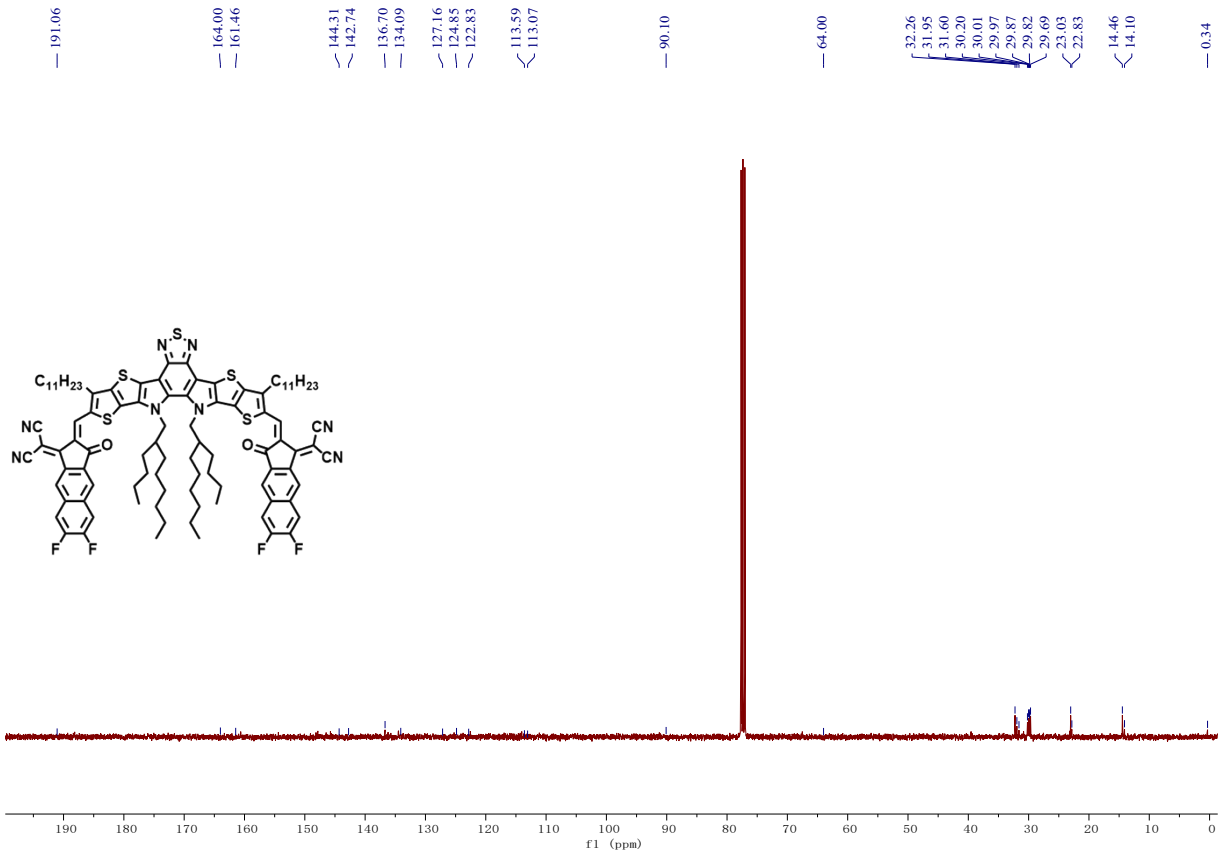

Figure S2. ^{1}C NMR of Y-TNF in $CDCl_3$.

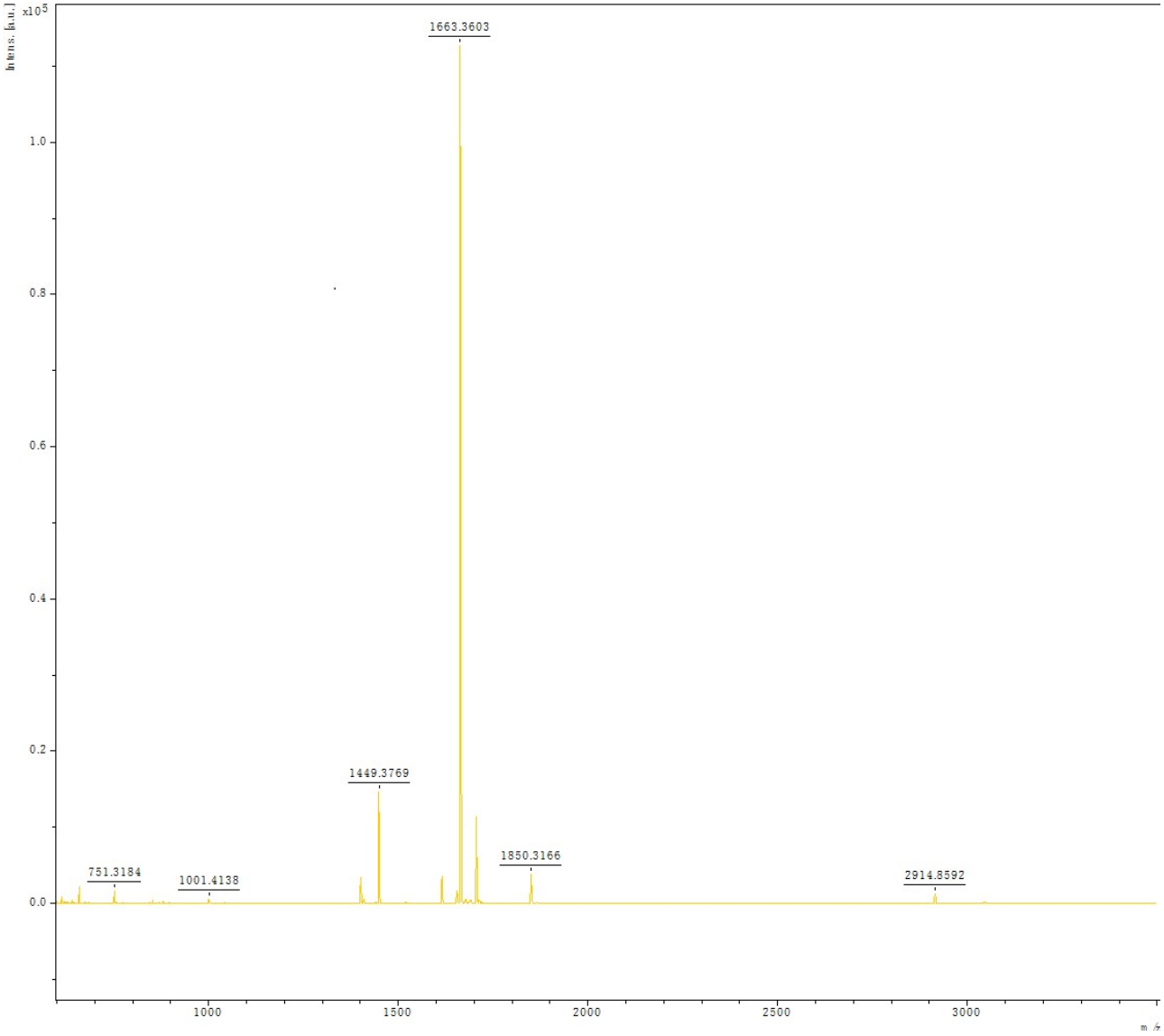

Figure S3. MALDI-TOF of Y-TNF.

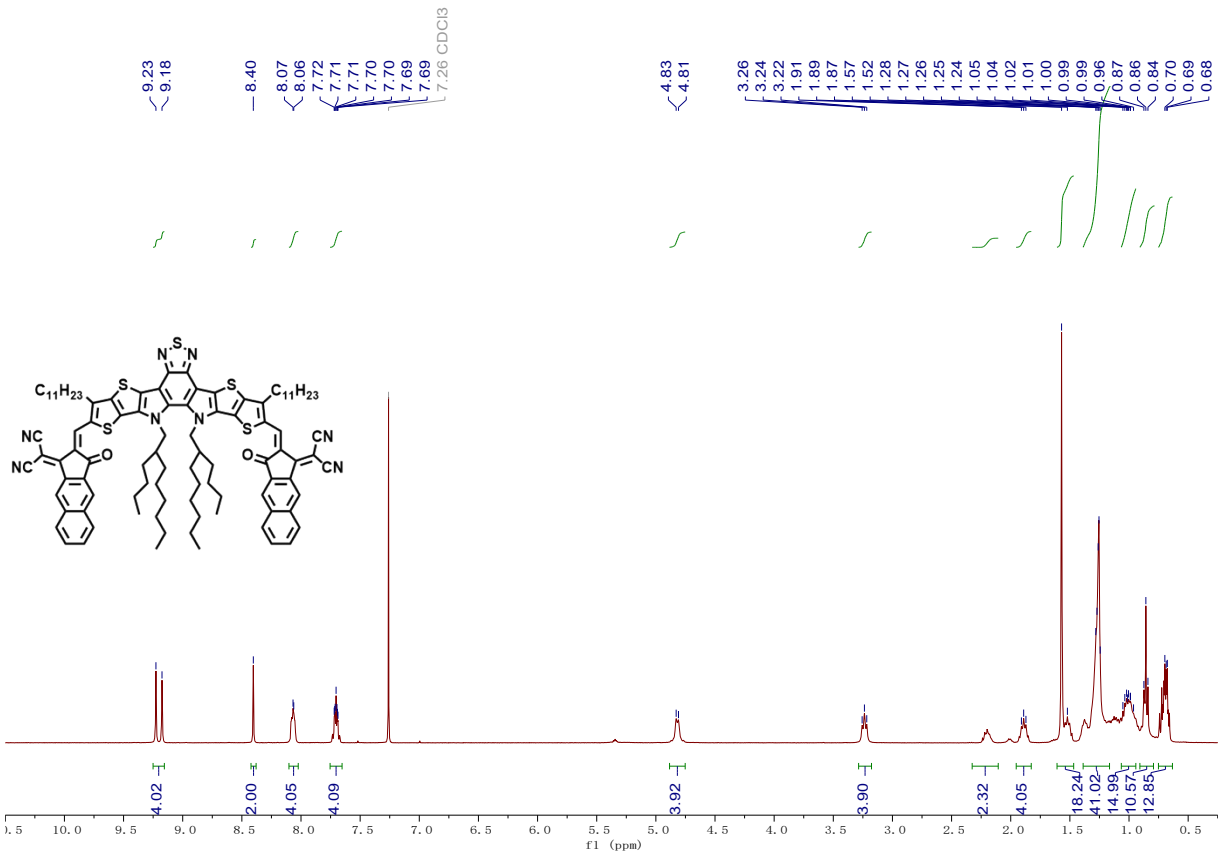

Figure S4. ^{1}H NMR of Y-TN in $CDCl_3$.

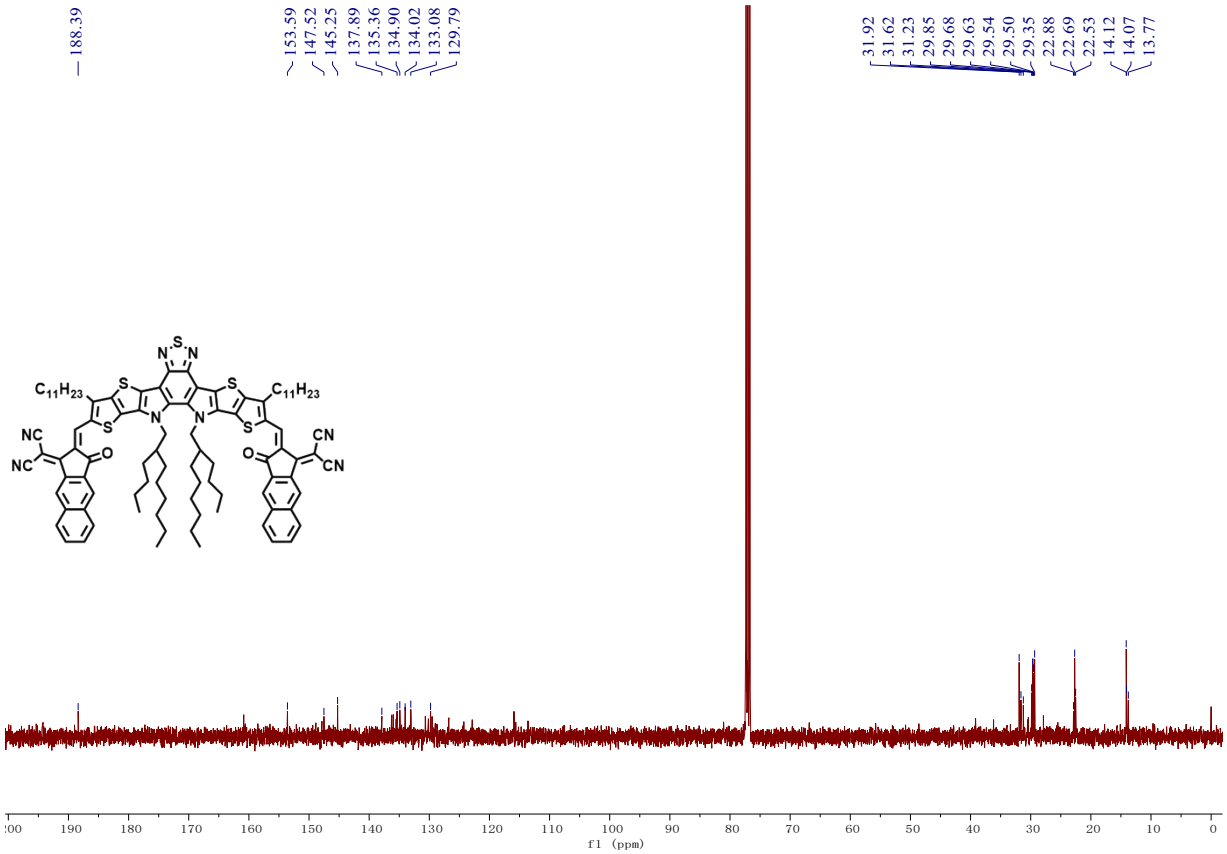

Figure S5. ^{1}C NMR of Y-TN in $CDCl_3$.

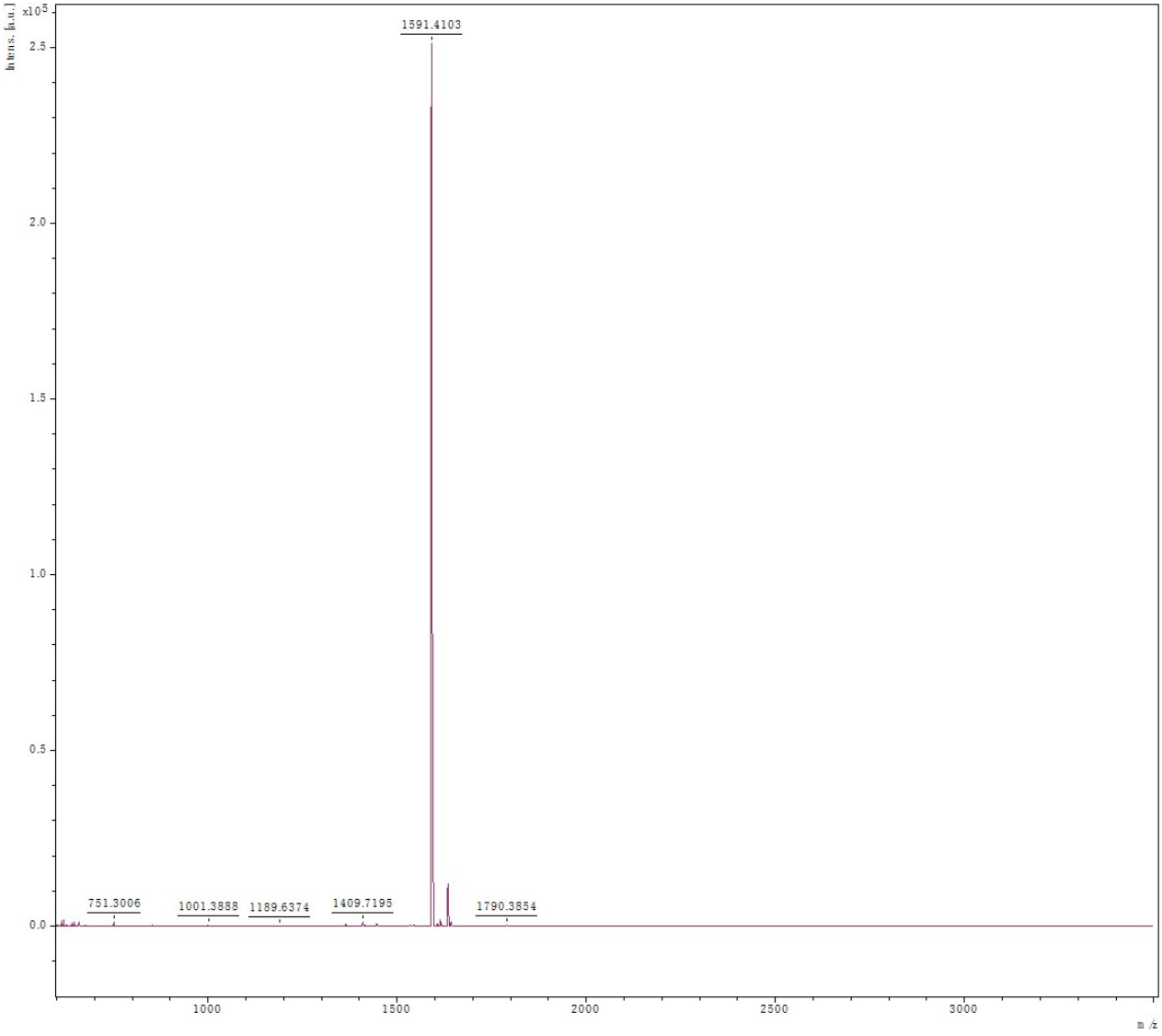

Figure S6. MALDI-TOF of Y-TN.

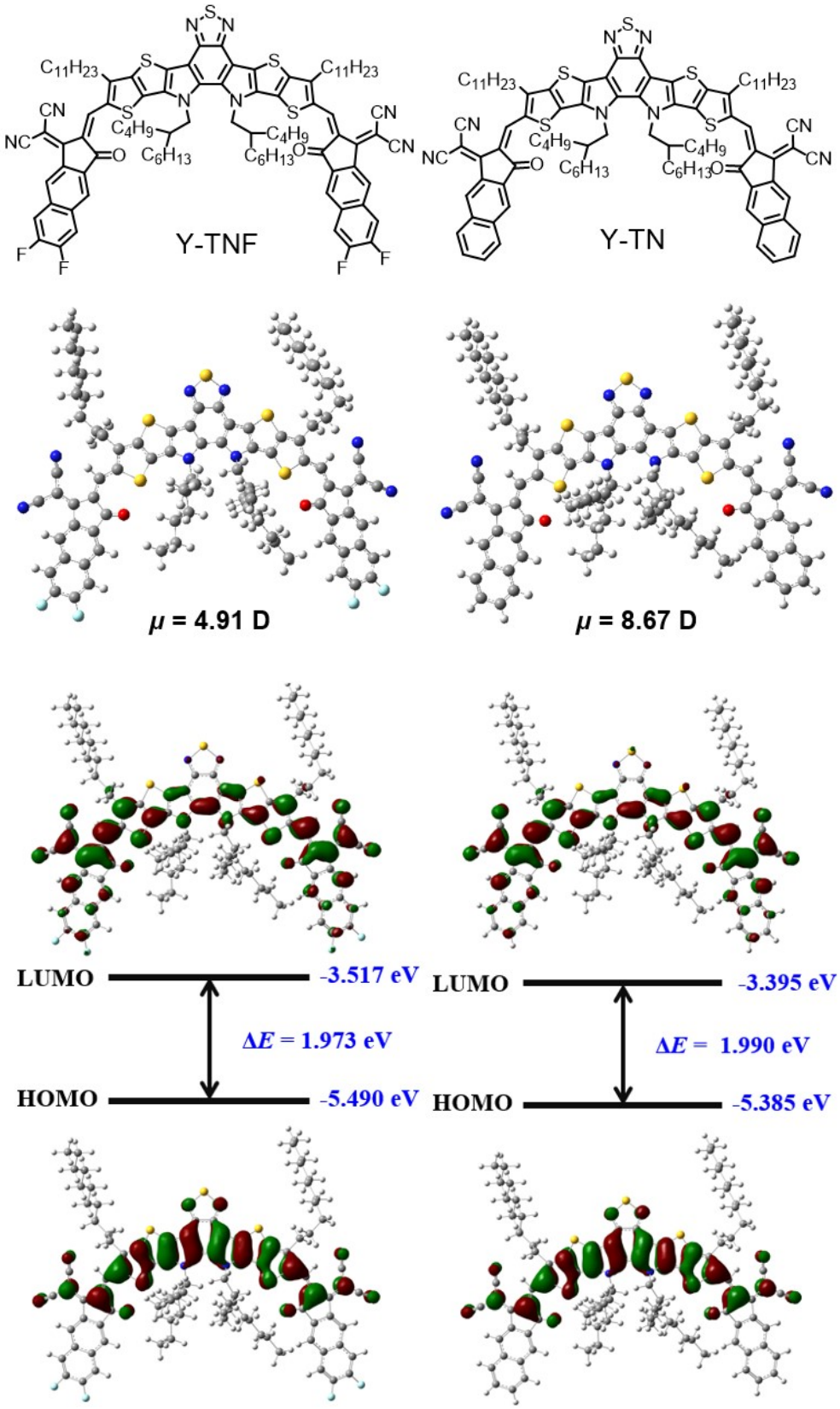

Figure S7. Chemical structures of Y-TNF and Y-TN, and the corresponding molecular conformations and electron cloud distributions of the frontier molecular orbitals based on DFT theoretical calculations at the B3LYP/6-31G(d,p) level.

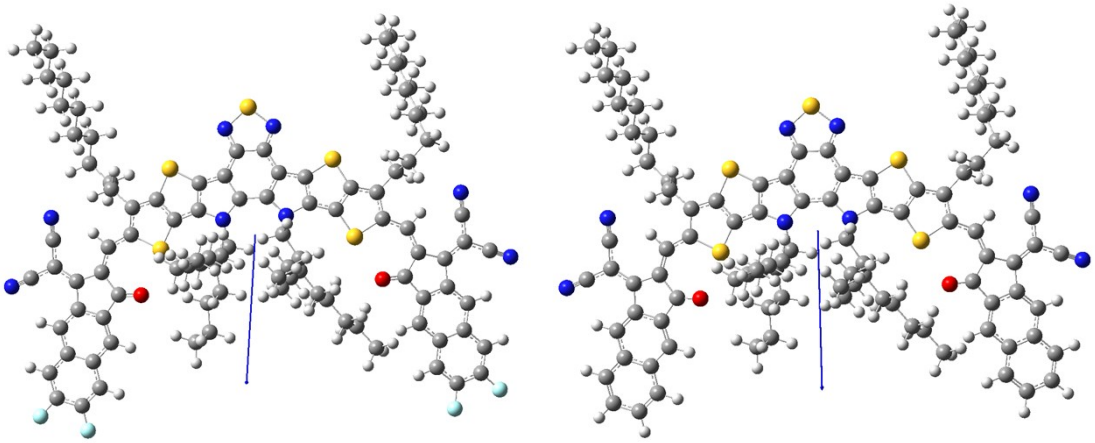

Figure S8. The corresponding Y-TNF (left) and Y-TN (right) dipole moment directions based on DFT theoretical calculations at the B3LYP/6-31G (*d*, *p*) level.

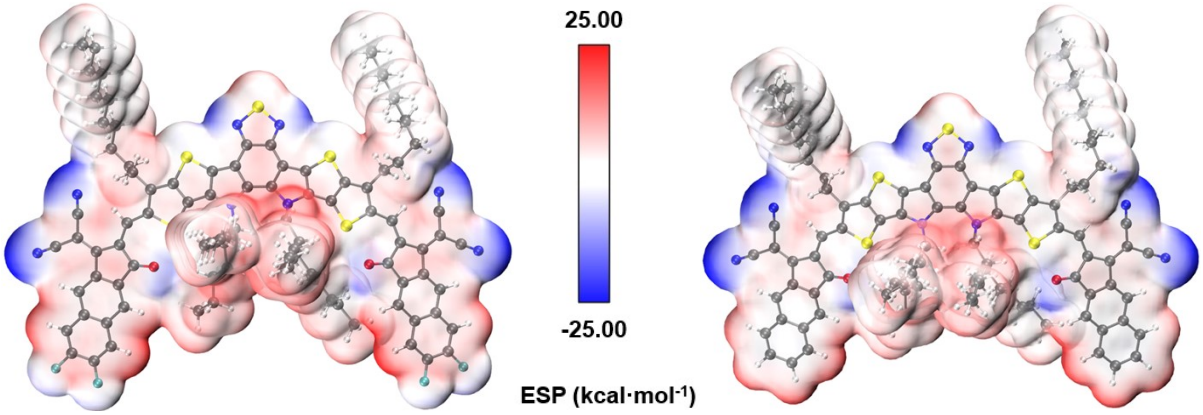

Figure S9. Electrostatic potential (ESP) of Y-TNF (left) and Y-TN (right).

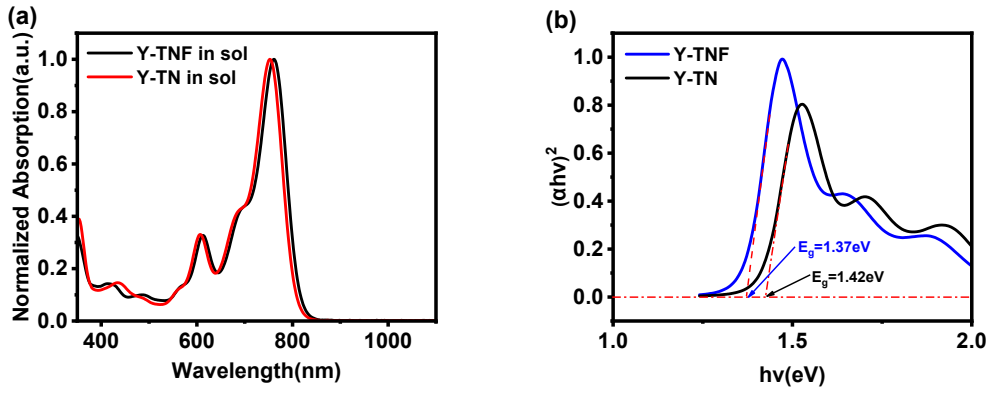

Figure S10. (a) UV-visible absorption curves of Y-TNF and Y-TN in chloroform solution, (b) optical band gaps of Y-TNF and Y-TN calculated from thin film UV absorption spectra.

Table S1. Optical and electrochemical properties of Y-TNF and Y-TN.

Material	UV-vis in solution		UV-vis in solid film			CV			Dipole moment (Debye)[a)]
	λ_{max} (nm)	λ_{edge} (nm)	λ_{max} (nm)	λ_{edge} (nm)	E_g^{opt} (eV)	HOMO (eV)	LUMO (eV)	E_g^{cv} (eV)	
Y-TNF	761	847	844	980	1.37	−5.54	−3.97	1.57	8.67
Y-TN	751	835	814	967	1.42	−5.46	−3.86	1.60	4.91

[a)] Obtained from gaussian theoretical simulation.

Table S2. GIWAXS parameters of the Y-TNF and Y-TN pure films.

Materials	**In plane (100)**			**Out of plane (010)**		
	Location (Å^{-1})	***d*-spacing (Å)**	**CCL (Å)**	**Location (Å^{-1})**	***d*-spacing (Å)**	**CCL (Å)**
Y-TNF	0.37	16.98	41.74	1.67	3.74	20.86
Y-TN	0.40	16.53	30.74	1.70	3.67	21.63

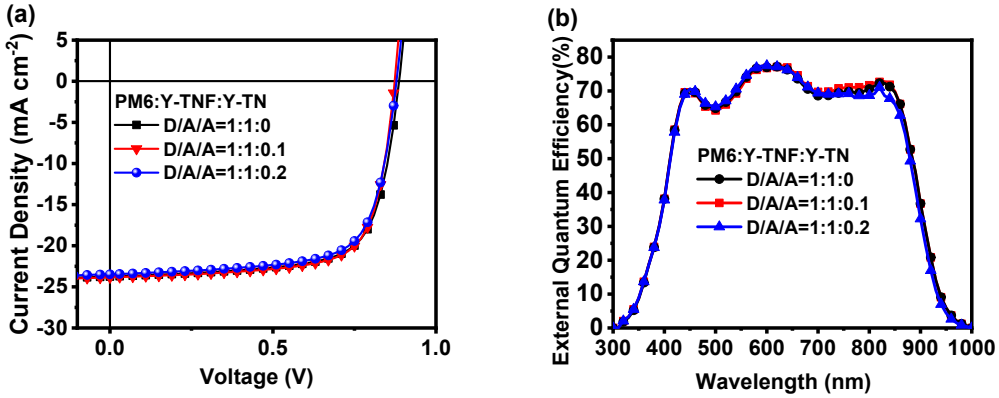

Figure S11. (a) *J-V* plots of PM6:Y-TNF:Y-TN-based OSCs with different D/A under the illumination of AM 1.5G, 100 mW cm^{-2}, (b) The corresponding EQE curves of the OSCs.

Table S3. Photovoltaic parameters of PM6:Y-TNF:Y-TN-based OSCs with different D/A under the illumination of AM 1.5 G, 100 mW cm^{-2}.

PM6:Y-TNF:Y-TN	V_{oc}(V)	J_{sc} (mA cm^{-2})	Cal. J_{sc} [a)] (mA cm^{-2})	FF(%)	PCE(%)
1:1:0	0.886	23.74	23.05	71.19	14.97
1:1:0.1	0.873	23.85	23.15	72.48	15.09
1:1:0.2	0.878	23.47	22.79	70.07	14.44

[a)] Integral J_{sc} from EQE curves.

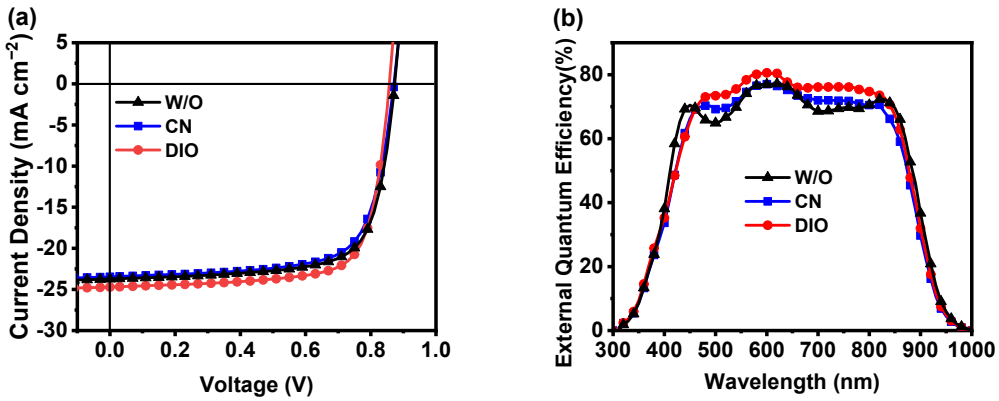

Figure S12. (a) *J-V* plots of PM6:Y-TNF:Y-TN-based OSCs (1:1:0.1, w/w/w) with different additive under the illumination of AM 1.5 G, 100 mW cm^{-2}, (b) The corresponding EQE curves of the OSCs.

Table S4. Photovoltaic parameters of PM6:Y-TNF:Y-TN-based OSCs (1:1:0.1, w/w/w) with different additive under the illumination of AM 1.5 G, 100 mW cm^{-2}.

Additive	V_{oc}(V)	J_{sc} (mA cm^{-2})	Cal. J_{sc} [a)] (mA cm^{-2})	FF (%)	PCE (%)
W/O	0.886	23.74	23.05	71.19	14.97
CN [a)]	0.871	23.47	22.79	71.25	14.57
DIO [b)]	0.856	24.70	23.98	74.29	15.71

[a)] CN is an abbreviation of 1-Chloronaphthalene, [b)] DIO is an abbreviation of 1,8-Diiodooctane.

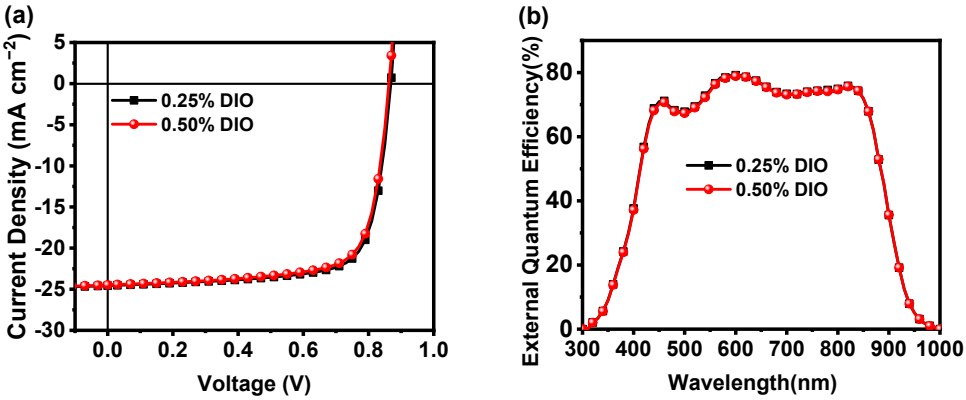

Figure S13. (a) *J-V* plots of PM6:Y-TNF:Y-TN-based OSCs (1:1:0.1, w/w/w) with different DIO contents under the illumination of AM 1.5 G, 100 mW cm^{-2}, (b) The corresponding EQE curves of the OSCs.

Table S5. Photovoltaic parameters of PM6:Y-TNF:Y-TN-based OSCs (1:1:0.1, w/w/w) with different DIO contents under the illumination of AM 1.5 G, 100 mW cm^{-2}.

PM6:Y-TNF:Y-TN	V_{oc}(V)	J_{sc} (mA cm^{-2})	Cal. J_{sc}[a)] (mA cm^{-2})	FF(%)	PCE(%)
0.25% DIO	0.868	24.57	23.85	74.77	15.95
0.50% DIO	0.862	24.48	23.77	74.05	15.63

[a)] Integral J_{sc} from EQE curves.

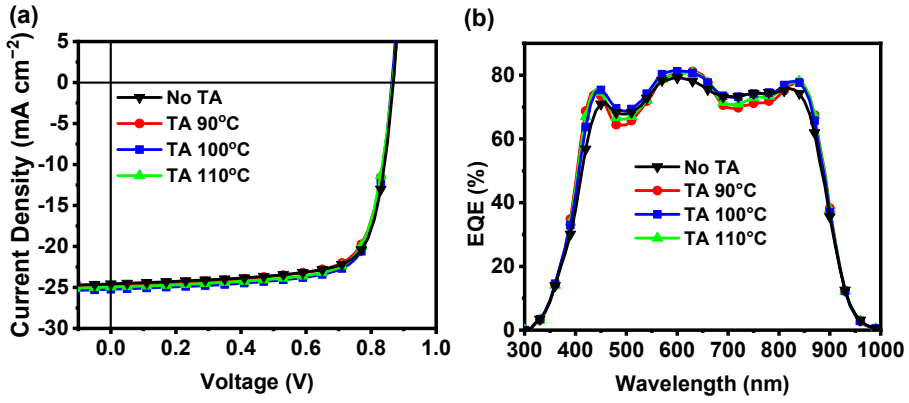

Figure S14. (a) *J-V* plots of PM6:Y-TNF:Y-TN-based OSCs (1:1:0.1, w/w/w) with different TA temperature for 10 min, 0.25% DIO as additive under the illumination of AM 1.5 G, 100 mW cm^{-2}, (b) The corresponding EQE curves of the OSCs.

Table S6. Photovoltaic parameters of PM6:Y-TNF:Y-TN-based OSCs (1:1:0.1, w/w/w) with different TA temperature under the illumination of AM 1.5 G, 100 mW cm^{-2}.

PM6:Y-TNF:Y-TN		V_{oc}(V)	J_{sc} (mA cm^{-2})	Cal. J_{sc}[a] (mA cm^{-2})	FF(%)	PCE(%)
0.25% DIO, TA 10 min	No TA	0.868	24.57	23.85	74.77	15.95
	TA 90°C	0.866	24.77	24.05	73.24	15.71
	TA 100°C	0.863	25.23	24.49	74.57	16.24
	TA 110°C	0.865	24.96	24.23	73.91	15.96

[a] Integral J_{sc} from EQE curves.

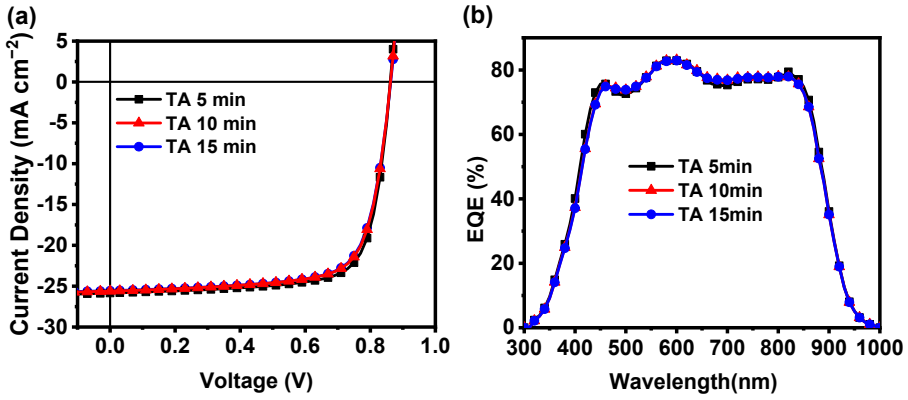

Figure S15. (a) *J-V* plots of PM6:Y-TNF:Y-TN-based OSCs (1:1:0.1, w/w/w) with different TA time, 0.25% DIO as additive and TA treatment at 100°C under the illumination of AM 1.5 G, 100 mW cm^{-2}, (b) The corresponding EQE curves of the OSCs.

Table S7. Photovoltaic parameters of PM6:Y-TNF:Y-TN-based OSCs (1:1:0.1, w/w/w) with different TA time, 0.25% DIO as additive and TA treatment at 100°C under the illumination of AM 1.5 G, 100 mW cm^{-2}.

PM6:Y-TNF:Y-TN		V_{oc}(V)	J_{sc} (mA cm^{-2})	Cal. J_{sc}[a] (mA cm^{-2})	FF(%)	PCE(%)
0.25% DIO, TA 100°C	5 min	0.857	25.84	25.10	75.10	16.63
	10 min	0.861	25.60	24.85	73.66	16.24
	15 min	0.862	25.55	24.80	73.40	16.17

[a] Integral J_{sc} from EQE curves.

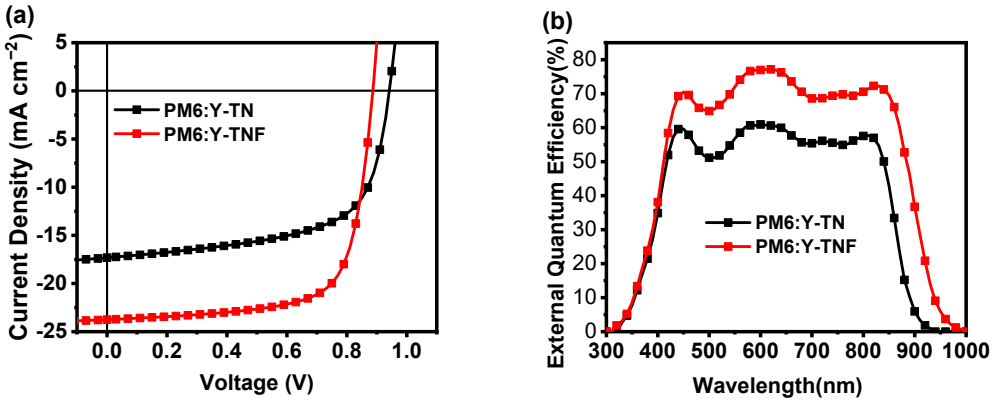

Figure S16. (a) *J-V* plots of the PM6:Y-TNF and PM6:Y-TN-based OSCs (1:1, w/w) with 0.25% DIO additive, and a TA treatment at 100°C for 5 min under an illumination of AM 1.5 G, 100 mW cm^{-2}, (b) EQE curves of the corresponding OSCs.

Table S8. Photovoltaic parameters of the PM6:Y-TNF and PM6:Y-TN-based OSCs (1:1, w/w) with 0.25% DIO additive, and a TA treatment at 100°C for 5 min under an illumination of AM 1.5 G, 100 mW cm^{-2}.

Active Layer	V_{oc} (V)	J_{sc} (mA cm^{-2})	Cal. J_{sc}[a)] (mA cm^{-2})	FF (%)	PCE (%)
PM6:Y-TNF	0.847	25.45	24.71	73.91	15.93
PM6 Y-TN	0.941	17.32	17.32	62.80	10.24

[a)] Integral J_{sc} from EQE curves.

Table S9. Parameters extracted from photo-CELIV plots.

Active Layer	A (V ms^{-1})	t_{max} (μs)	Δj (mA)	$j(0)$ (mA)	$\Delta j/j(0)$	d (nm)	μ[a)] (cm^2 V^{-1}s^{-1})
PM6:Y-TNF	72.5	1.704	3.276	1.952	1.678	100	1.97×10^{-4}
PM6:Y-TNF:Y-TN	72.5	1.676	3.496	2.099	1.666	100	2.05×10^{-4}

[a)]Calculated from the formula, $\mu = 2d^2/[3At_{max}^2(1+0.36\Delta j/j(0))]$, where d is the active layer thickness, A is the voltage ramp, t_{max} is the maximum current time, Δj is the peak transient current, and $j(0)$ is the displacement current.

Table S10. GIWAXS parameters of the PM6:Y-TNF and PM6:Y-TNF:Y-TN films.

Materials	In plane (100)			Out of plane (010)		
	Location ($Å^{-1}$)	***d*-spacing (Å)**	**CCL (Å)**	**Location ($Å^{-1}$)**	***d*-spacing (Å)**	**CCL (Å)**
PM6:Y-TNF	0.30	20.93	64.89	1.66	3.78	21.63
PM6:Y-TNF:Y-TN	0.30	20.26	53.09	1.71	3.67	20.86